Research in Art and Archaeology: Capabilities and Investigations at the Australian Synchrotron

H. E. A. Brand,[1] D. L. Howard,[1] J. Huntley,[2] P. Kappen,[1] A. Maksimenko,[1] D. J. Paterson,[1] L. Puskar,[3] and M. Tobin[1]

[1]*Australian Synchrotron, ANSTO, Clayton, Victoria, Australia*
[2]*Griffith University, Gold Coast Campus, Queensland, Australia*
[3]*Helmholtz-Zentrum Berlin, Berlin, Germany*

Introduction

In the Australian Synchrotron's short history we have made some important advances in instruments and capabilities that can be employed to study art and archaeology. In this article we describe the capabilities at the Australian Synchrotron that are well-suited to investigating art, archaeology and cultural heritage. We also present some case studies that demonstrate the breadth and impact of science that has been performed by researchers using these capabilities.

Synchrotron radiation has many advantages that make it ideally suited to investigating art, archaeology and cultural heritage. The broad spectrum of radiation that can be employed and in particular the penetrating nature of the radiation at hard X-ray energies give the ability to conduct 3D reconstruction with tomography. In many cases the techniques can be non-destructive and performed in-situ. The intense infrared radiation allows infrared microscopy at diffraction limited resolution and the recently developed attenuated total reflection mode can probe the surface of very delicate samples.

Below we describe the relevant beamlines, their capabilities, and then illustrate with some key examples of research, from paleobotany to the investigation of paintings.

Overview of techniques available at the Australian Synchrotron

Infrared Microscopy (IRM)

Infrared Microscopy can provide spatially resolved spectroscopic information on organic and inorganic compounds. The combination of high brilliance and collimation of the synchrotron beam enables high signal-to-noise ratios at diffraction limited spatial resolutions between 3-8 µm, making the Infrared Microspectroscopy (IRM) beamline ideally suited to the analysis of microscopic samples e.g. small particles, thin films and layers within complex matrices, as well as single cells and complex biological systems.

The IRM beamline can also employ Attenuated Total Reflection (ATR). ATR relies on a form of internal reflection to enable the analysis of more difficult samples with IR spectroscopy, e.g. samples that cannot be microtomed for transmission measurements or that do not adequately reflect IR for reflection. Compared to transmission and reflectance FTIR, ATR offers the advantage of enhanced spatial resolution below the diffraction limit.

X-ray Fluorescence Microscopy (XFM)

The beamline has two probes optimised for studies at length-scales spanning two orders of magnitude. A milliprobe has a resolution of around 50 µm and a Kirkpatrick-Baez mirror microprobe is optimised for applications requiring high flux at the micron length scale. These systems can be

used to obtain maps of elemental distribution and for a range of spectroscopic applications such as determining oxidation state and speciation. The fast data acquisition schemes enable 3D measurements such as XRF tomography and XANES imaging.

Powder Diffraction (PD)

The Powder Diffraction beamline is located on a bending magnet source and has been designed to operate over the energy range 8-21 keV. The beamline consists of two experimental hutches and a user cabin. Experimental hutch one is designed for sample capillary analysis, and experimental hutch two is for specialised user setups, and those requiring a 2D detector.

The range of techniques available at the PD beamline that are relevant to cultural studies to include: Ab initio structure solution, in situ examination of chemical and mineralogical processes, structure/property studies, parametric studies, including variable temperature, phase identification and quantification and examination of stress and strain.

X-ray Absorption Spectroscopy (XAS)

The first experimental station is optimised for transmission and fluorescence XAS on standard samples. This hutch supports the use of transmission ionization chambers, a 100 element solid state Ge fluorescence detector, a PIPS detector, Soller slits and filters, a fast beam shutter, a 10 K cryostat, capillary heating, and a room temperature sample stage. The second experimental station is designed to allow and user supplied sample environments and non-standard samples.

Imaging and medical beamline (IMBL)

The imaging and radio-biology techniques available on the IMBL include: Phase-contrast (propagation based) x-ray imaging, which allows much greater contrast from weakly absorbing materials such as soft tissue than is possible using conventional methods; Two and three-dimensional imaging at high resolution (10 µm voxels); Lower doses than conventional x-ray methods, making longitudinal studies (serial imaging) possible; Tuneable beam energy with bandwidth of $< 10^{-3}$ enabling imaging of specific elements with very high sensitivity, possibly down to micron scales.

More details on the current and future beamlines at the Australian Synchrotron can be found on our website [1].

Palaeobotany

Siliceous permineralized peats of Lopingian (late Permian) age are known from several sites within foreland basins along the eastern margin of Gondwana [2–4]. Many of these peat deposits are associated with ash-fall tuffs sourced from felsic to intermediate volcanism that developed along the convergent Panthalassan margin of Gondwana and Cathaysia at the end of the Palaeozoic. These deposits are prized for hosting exceptional three-dimensionally preserved plant fossils that help elucidate the anatomy, physiology, and autecology of the entombed vegetation, together with providing insights into interactions with fungi and terrestrial arthropods. The permineralized fossils also provide insights into the organic connections between normally isolated plant organs, and the contents of entombed microsporangia yield information on the intraspecific variability of normally dispersed spores and pollen. The onshore Sydney Basin of eastern Australia hosts a 14500-m-thick Permian-Triassic mixed marine and fluvial succession that locally hosts world-class bituminous coal resources [5, 6]. Individual transported and in situ silicified woody stumps and logs, and cherty

tuffaceous beds with leaf impressions, are relatively common in Lopingian strata throughout the basin [7]. On this basis, there are strong prospects that additional Permian silicified peat deposits will come to light elsewhere in the Sydney Basin.

We document a case of a transported cobble of siliceous permineralized peat probably derived from Lopingian strata of the southern Sydney Basin. The peat contains a range of anatomically preserved plant fossils such as seeds (Figure 1) [8]. Permineralized peats are especially significant in that they preserve the three-dimensional architecture of the mass of organic matter that contributed to the formation of coal. Adpression assemblages are typically preserved in clastic-rich flood basin deposits and do not necessarily provide an accurate representation of the coal-forming plant community. Petrographic analyses of bituminous coals can provide useful quantitative information on the range of plant tissue types contributing to the organic accumulation, but it is usually impossible to identify specific plant taxa or organs in such studies.

Palaeoarchaeology

The Ertebølle shell middens or kitchen middens (kjøkkenmodding) of Denmark are well studied [9]. These middens comprise layers of discarded mollusc shells, mainly oysters (Ostrea edulis) but also other species such as cockles (Cerastoderma edule) and blue mussels (Mylitus edulis), and are mixed with cultural remains. Kitchen middens always lie directly on and along prehistoric shorelines, close to natural shell banks and always at good “fishing-localities”. Following glacio-isostitic adjustments and post-glacial rise, many of these middens in the south of Denmark were submerged and can be found at shallow depths, perhaps the most famous associated with the settlement of Tybrind Vig. Another such site is that of Hjarnø Sund, located in a water depth of 0.5–2 m on the western shore of the small island of Hjarnø in Horsens Fjord [10]. Underwater excavation and sediment coring of this site undertaken between 2013 - 2017 has revealed with CT scanning (Figure 2) shell deposits and a rich collection of cultural material (including worked flint, fish and mammal bone, antler and wood), ranging in age from the Early Ertebølle (~ 7300 ka) to the Middle Ertebølle (~ 6500 ka).

The general formation history of the Hjarnø shell midden site has been documented [10], and describes the accumulation of shell debris on a sloping site adjacent to a remnant lake or brackish swamp before being submerged, with further submerged shell deposits noted further north along the coast either as a separate midden or part of a continuum. As the water level deepened, the swamp would have transitioned into an open marine environment. Nearshore coastal processes would have resulted in sediment accumulating over the (gyttja) peat forming intertidal beach and subtidal sand banks and shoals a little further offshore. This study adds a new context to the emerging literature on the application of micromorphology and CT scanning to archaeological sciences [11–15].

Rock art

FTIR microspectroscopy

The Dalakngalarr 1 site in Jawoyn Country, Arnhem Land, is the location of a large collection of Australian aboriginal rock art, which includes many paintings of animals such as fish, turtles and macropods, in the distinctive “X-ray” style, in which the internal structures of the animals are depicted (Figure 3). The animals are painted in various shades, including red and yellow, plus a less common purple pigment. Elemental analysis by SEM-EDS revealed some differences in composition, including higher levels of K, Mg and S in the red pigment, with all three pigments containing Al, Si and Fe, typical of ochres. Small particles of each pigment were analysed by FTIR microspectroscopy

at the IRM beamline, by compressing the particles between two diamonds to reduce sample thickness to below 10 μm, and then focusing the IR beam on selected components of 5 μm x 5 μm within the particle [16]. The IR spectra from the red and yellow pigments were broadly similar, indicating the presence of kaolinite, goethite and hydrated magnesium oxalate, while the O-H stretching and deformation bands (3400 cm^{-1} and 800 cm^{-1}) indicated the presence of poorly crystallised "protohaematite" (Figure 3). A combination of Raman spectroscopy and FTIR microspectroscopy confirmed the absence of water and the presence of haematite in the purple pigment, while the Raman spectroscopy revealed the absence of a previously reported "disorder band", which is known to be lost when haematite is heated. These combined resulted led to the conclusion that the purple pigment was likely produced, either deliberately or inadvertently, by the heating of an original ochre.

Powder Diffraction

Powder diffraction is often rejected as a technique for studying cultural heritage materials as traditional powder diffraction laboratory instruments often require a larger volume of sample for an analysis than is reasonable when compared to the cultural value of the item. Add to this that the sample must, in most cases, be ground to create a powder and it quickly becomes very unattractive.

Synchrotron powder diffraction however, only requires, at minimum, 2-3 mg to obtain a high-quality pattern. The added resolution and signal to noise of the synchrotron X-ray beam and the detectors available at the synchrotron also makes them much more sensitive to minor phases than in a laboratory setting.

The ritually repainted Wandjina motifs of the Kimberly in north west Australia provide a unique opportunity for researchers to investigate the past cultural landscapes, how the geographic origin of pigments, as well as their recipes have changed[17, 18]. A pilot study [19], took paint flecks from discrete layers within a stratified paint chip, top of Figure 4 taken from the eye of a larger Wandjina motif, bottom of Figure 4.

The layers are mineralogically distinct whilst conforming to existing bulk measurements as a whole. Sensitivity to minor phases proves imperative when studying the effects of the subtropical climates of northern Australia with a view to preservation of these important cultural sites.

Investigation and analysis of paintings

X-ray fluorescence microscopy

X-ray fluorescence (XRF) microscopy is an imaging technique used to determine spatially resolved elemental composition. The X-ray fluorescence microscopy (XFM) beamline [20] has been involved in the analysis of cultural materials for a decade. The beamline's particular strength is in the detection of metals. Depending on the application, the spatial resolution used typically ranges from approximately 1 – 100 μm, with the finest resolution provided by a set of Kirkpatrick-Baez mirrors. The Maia 384 detector array is the primary XRF detector [21] - its zero readout overhead and large detection solid angle has made it an important tool in the rapid analysis of cultural heritage.

Synchrotron XRF is well suited to the analysis of cultural heritage. XRF is non-destructive and can be used non-invasively with little to no sample pre-treatment. It is relatively fast and can detect multiple elements in a single measurement. The advantages of synchrotron radiation relative to a laboratory X-ray source are its narrow bandwidth, its brilliance, and the tunability of the incident energy.

Energy tunability permits selective excitation of elements. A common issue in the XRF analysis of vintage paintings is the high concentration of lead in pigments, which can lead to excessive XRF counts on the detector and thereby limiting sensitivity to other elements present in lesser amounts. Scanning with an excitation energy below the lead L_3 edge (13.035 keV) can be done to avoid a high lead fluorescence signal [22]. This energy selectivity was used in the analysis of a Tudor painting of Henry VIII for example [23]. Energy tunability also enables analysis of elemental speciation and local atomic coordination information. Elemental mapping as a function of the incident energy across an element's absorption edge, known as XANES imaging or chemical state imaging, was used to investigate the darkening of chrome yellow pigments in some works of van Gogh [24]. Chromium in these pigments can degrade from the original hexavalent state (yellow) to the trivalent state (brown), and the chemical state imaging method can spatially resolve these differences in oxidation state.

The ability to reveal metal distributions in the pigments of paintings is an area where fast scanning XRF excels. Pigments from Palaeolithic cave art samples were characterised at XFM to complement other analytical methods. Here small flakes (>2 mm) of rock art paints adhered to limestone were analysed, revealing the pigment's iron-based composition [25]. Aboriginal artefacts [26] have been non-invasively studied at XFM to provide insight to the application of natural mineral pigments versus commercially made or modern pigments.

An example oil painting scanned at the XFM beamline is shown in Figure 5(a) with an overlay of three elemental maps in Figure 5(b). In this example the whole painting was scanned in one hour. The overlapping areas of copper and bromine, which appear as yellow and orange on the composite elemental map in Figure 5(b), strongly suggest the presence of a pigment called Pigment Green-36, a brominated copper phthalocyanine compound. In many cases, the penetrating ability of the characteristic X-rays has proven advantageous, often permitting the observation of "hidden" images painted beneath the surface layer. Observing underlying images provides valuable insights into artworks and artist's technique. Australian artists have featured heavily at XFM. The analysis of a painting by Arthur Streeton [22] exposed a hidden self-portrait, a work by Sidney Nolan [27] revealed a portrait under one of his signature 'Ned Kelly' masks, and a large painting by Frederick McCubbin [28] showed his many changes or pentimenti before the final composition. Examination of Edgar Degas' *Portrait of a Woman* is another case in point, where a hidden portrait of a woman was clearly revealed with synchrotron XRF imaging, which could not be resolved with conventional methods such as X-ray radiography or infrared imaging [29].

To enable the safe and efficient analysis of large objects such as paintings, a dedicated custom-designed scanning station known as the milliprobe has been installed at the XFM beamline [30], Figure 5(c). The milliprobe has the ability to scan objects having a mass up to 15 kg over an area 600 mm × 1100 mm at a maximum speed of 175 mm/s. The time required to mount a painting is several minutes. The beam size for the milliprobe is defined by a set of X-ray beam slits and the finest spatial resolution is approximately 50 µm, with standard scans performed at 100 µm pixel size. The short dwell times follows the principle of keeping radiation dose levels as low as reasonably achievable, which is important for objects where radiation damage is a major concern. The raster scanning control system incorporates a parabolic (kinematically optimised) trajectory that minimises end of line turnaround, further reducing time overheads.

In summary, large area, high definition scanning XRF is a powerful tool for the elemental analysis of a diverse range of cultural heritage objects. It can both show fine details and maintain the overall context of the sample, which is extremely useful and significantly reduces guesswork in the interpretation of the data.

FTIR microspectroscopy

Metal soaps, in particular palmitates and stearates, have been implicated in the degradation of significant artworks, whereby they can form as a reaction between metal ions from pigments and fatty acids in oil-based binding media. Zinc oxide, in use in paints since the 1840s, is particularly susceptible, in particular when used in combination with the contemporary paint additive aluminium stearate. Laboratory-based FTIR spectroscopy and synchrotron FTIR microspectroscopy were used to study a series of prepared paint films, aged for between 11 and 32 years [31]. Laboratory FTIR revealed differences between the outer (exposed) and lower (unexposed) surfaces of the paint films, with a broad zinc carboxylate absorbance peak between 1560 cm^{-1} and 1620 cm^{-1} detected from the upper surface, while a narrower peak between 1535 cm^{-1} and 1545 cm^{-1} was indicative of crystalline zinc stearate from the lower surface. Synchrotron FTIR microspectroscopy 2D mapping was used to help understand the formation, migration and aggregation of the zinc stearate and other carboxylates within 5 μm thick microtomed paint cross sections flattened onto an IR-transparent diamond window. The 2D maps were able to expose concentrations of metal carboxylates at discrete locations within the sections, including dispersed clusters of aluminium stearate, and also accumulations of zinc stearate which had formed and crystallised in situ (Figure 6). These maps reveal gradients in the concentration of zinc carboxylates when formed in the presence of aluminium stearate, while appearing as more dispersed clusters when aluminium stearate was absent. The observed phase separation of zinc stearate has important implications for the long-term stability of paintings.

Conclusions and outlook

There is a powerful suite of techniques and a strong program of research at the Australian Synchrotron focussed on art, archaeology and cultural heritage studies. Looking to the future, there are a number of new beamlines being constructed under the BRIGHT project including Micro-Computed Tomography, Medium Energy X-ray Absorption Spectroscopy, Advanced Diffraction and Scattering and X-ray Fluorescence Nanoprobe that will enhance and expand the capabilities at the Australian Synchrotron for research in art and archaeology.

Acknowledgements

For the powder diffraction studies of rock art, we acknowledge the traditional custodians of the central Kimberley, the Ngarinyin people, from whose Country and culture the sample analysed originates. Part of this research was undertaken on the IMBL, IRM, PD, and XFM beamlines at the Australian Synchrotron, part of ANSTO.

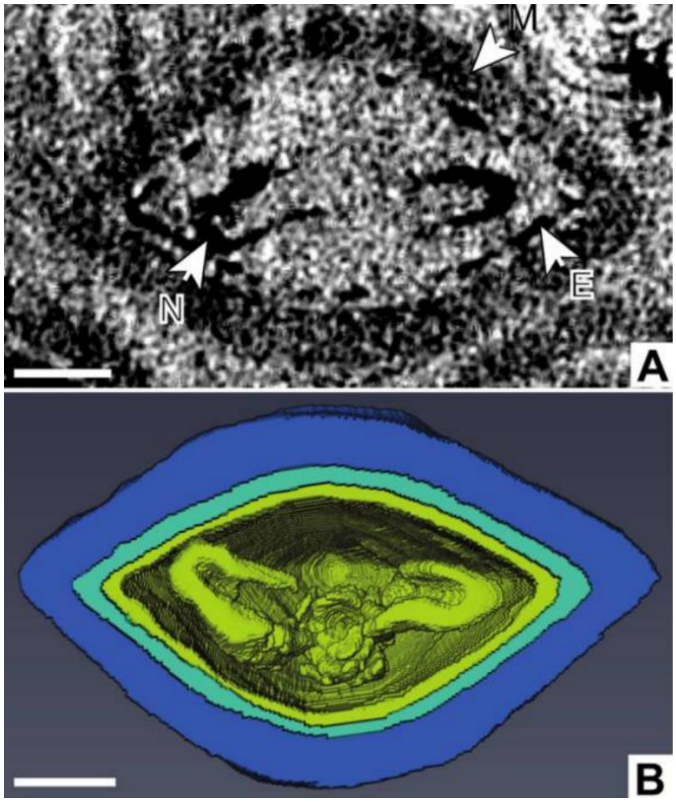

Figure 1: (a) X-ray synchrotron tomographic reconstructions of the seed Illawarraspermum ovatum, Medial transverse section (M - mesotesta; N - nucellus; E - endotesta); (b) Medial transverse section of rendered volume, basal view, colored volumes correspond to those labelled in (a).

Figure 2: (Left) Slice through resin-impregnated section of midden used for thin section preparation. (Right) 3D render of the stronger attenuating material (mainly shell, flint) in the resin block as viewed with the synchrotron.

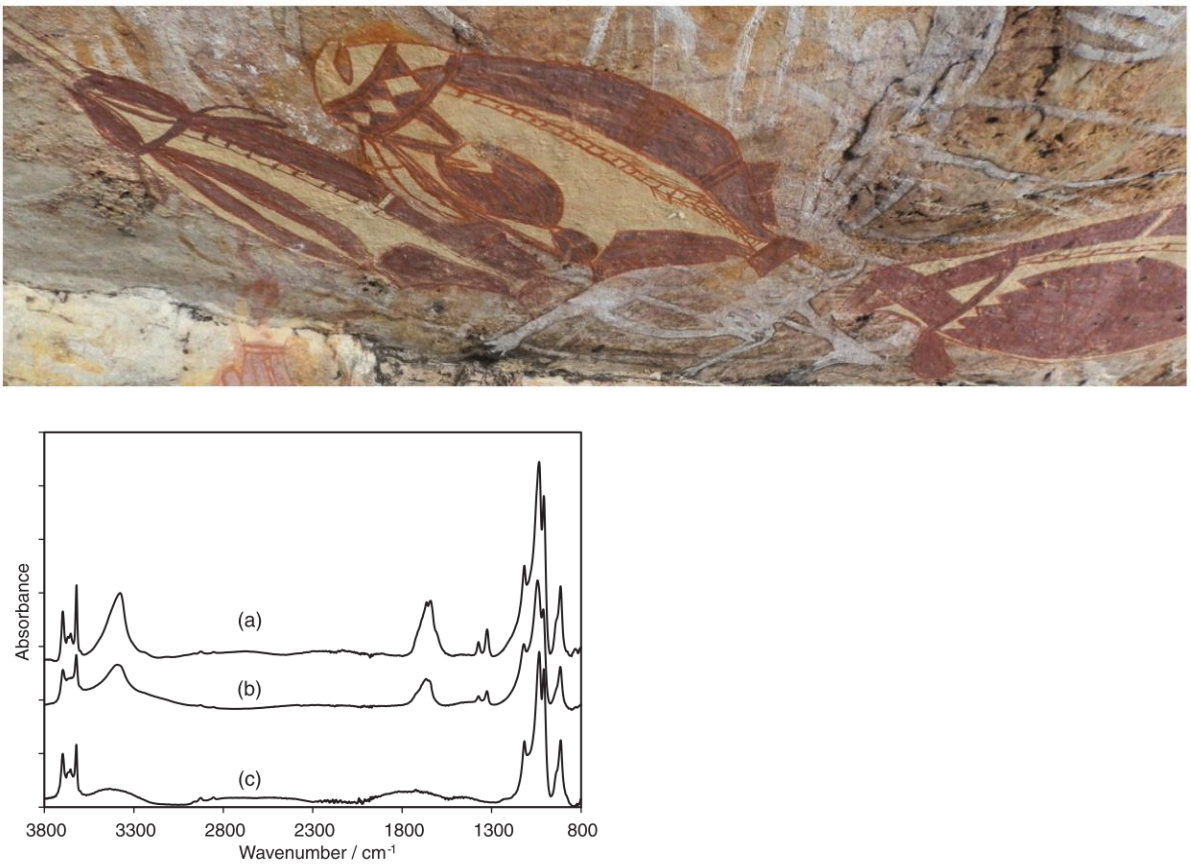

Figure 3: (Top) Rock art sampling region, red pigment as outline, yellow pigment and purple pigment as infill (photograph by Paul Thomas). (Bottom) Infrared spectra of pigments (a) yellow (b) red, and (c) purple.

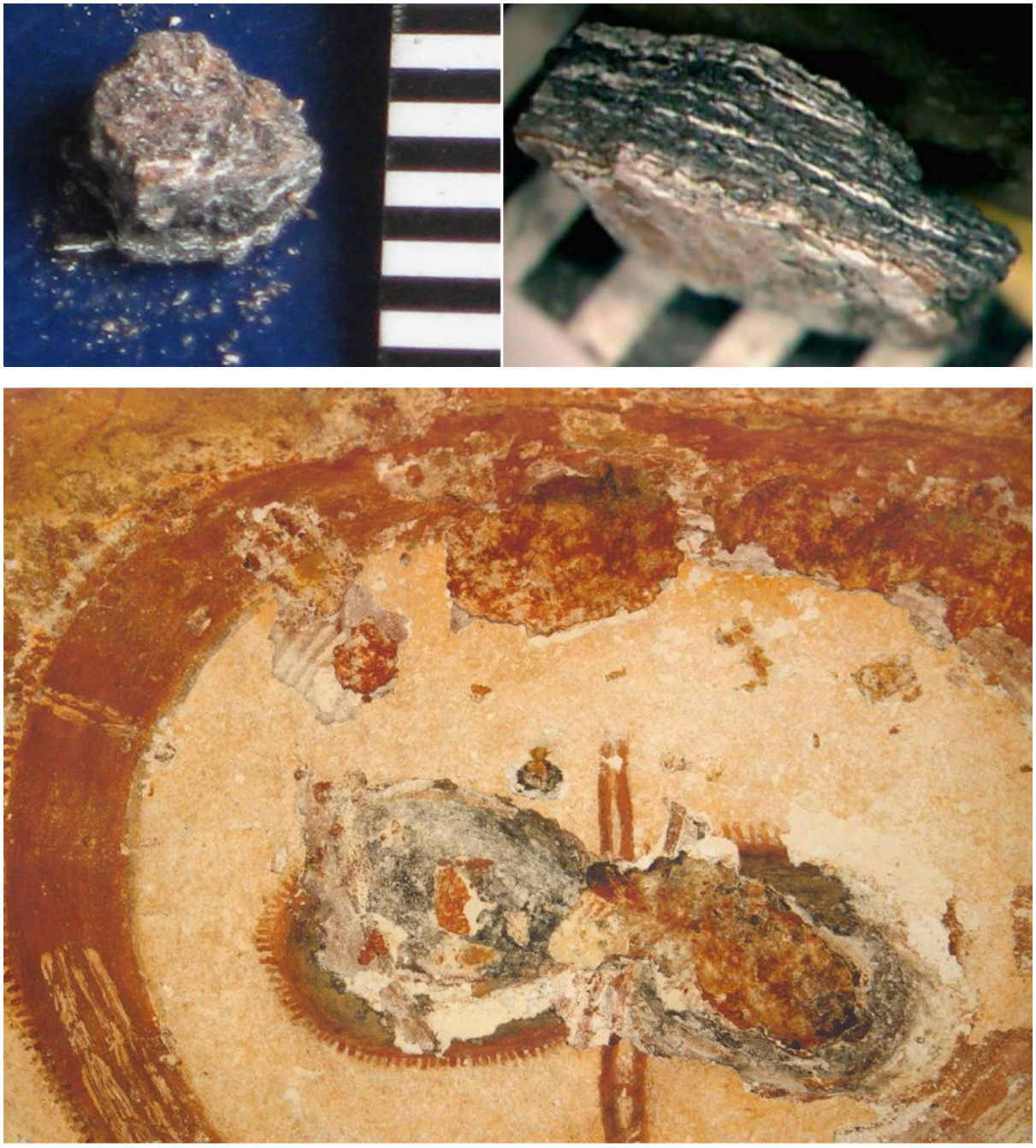

Figure 4: (Top) Wandjina paint flake analysed in the pilot powder diffraction study. (Left) overview; (Right) profile. The small detached flecks in the left image include the subsamples analysed. Note the scale is in millimetre increments. (Bottom) Wandjina site at the King Edward River crossing showing flake exfoliation typical of that described in the text (photograph by Mike Donaldson, reproduced from [32] *with permission).*

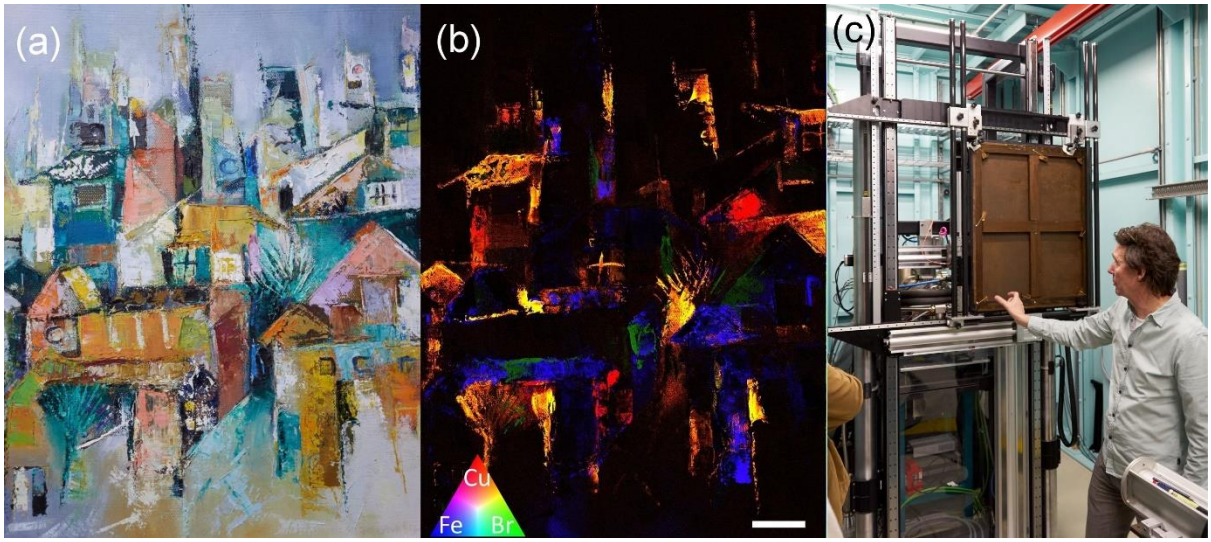

Figure 5: An example of X-ray fluorescence elemental mapping: (a) Visible light image of mid-twentieth century oil painting on canvas, artist unknown; (b) XRF elemental map composite image showing the distribution of copper (red), bromine (green) and iron (blue). Scan area 511 × 397 mm^2, 0.4 mm pixel size, 60 minute scan time. Scale bar = 50 mm; (c) preparing to scan a painting with the milliprobe apparatus at XFM beamline.

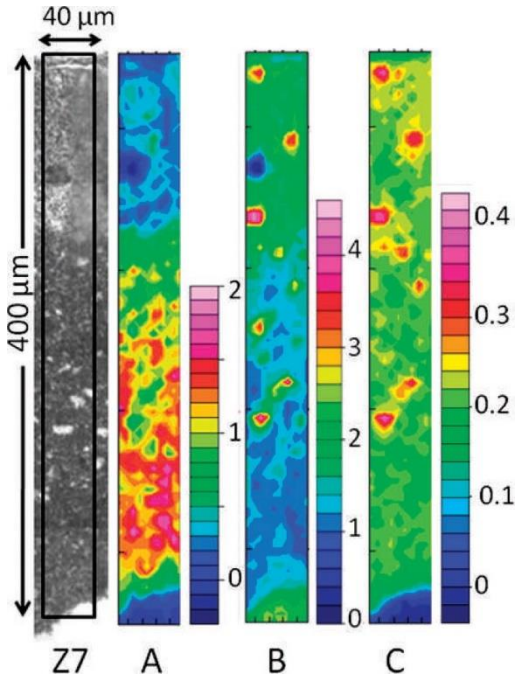

Figure 6: (Left) Light microscope image of Zinc White Control with safflower oil and aluminium stearate IR absorption maps showing distribution of (A) zinc carboxylate 1525–1555 cm^{-1}, (B) broad carboxylate 1560–1620 cm^{-1}, and (C) aluminium stearate 1585–1595 cm^{-1}. Figure adapted from [31].

References

1. Australian Synchrotron Beamlines at <https://www.ansto.gov.au/user-access/instruments/australian-synchrotron-beamlines>
2. J. M. Schopf, *Antarct. J.* **5**, 62 (1970).
3. R. E. Gould and T. Delevoryas, *Alcheringa An Australas. J. Palaeontol.* **1**, 387 (1977).
4. K. Pigg and S. McLoughlin, *Rev. Palaeobot. Palynol.* **97**, 339 (1997).
5. D. Agnew et al., Sydney Basin - Newcastle Coalfield, Geological Society of Australia, 197–212 (1995).
6. N. Z. Tadros *Wollongong Thesis Collect.* (1995). <http://ro.uow.edu.au/theses/840>
7. C. F. K. Diessel, *Fuel* **64**, 1542 (1985).
8. S. McLoughlin, A. Maksimenko, and C. Mays, *Int. J. Plant Sci.* **180**, 513 (2019).
9. S. H. Andersen, *Proc. Prehist. Soc.* **66**, 361 (2000).
10. C. Skriver et al., Hjarnø Sund: An Eroding Mesolithic Site and the Tale of two Paddles, (2017). doi:10.1007/978-3-319-53160-1_8
11. W. P. Adderley et al., *Archaeol. Prospect.* **8**, 107 (2001).
12. S. Hughes, CT Scanning in Archaeology, in *Computed Tomography - Special Applications*, Edited by L. Saba, IntechOpen (2011), 57–70. doi:DOI: 10.5772/22741
13. K. Haneca et al., *Archaeometry* **54**, 893 (2012).
14. D. J. Huismanet al., *J. Archaeol. Sci.* **49**, 585 (2014).
15. D. J. M. Ngan-Tillard and D. J. Huisman, Micro-CT Scanning, (2017). doi:10.1002/9781118941065.ch42
16. A. Hunt, P. Thomas, D. James, B. David, J.-M. Geneste, J.-J. Delannoy, and B. Stuart, *Microchem. J.* **126**, 524 (2016).
17. I. M. Crawford and R. Penrose, The art of the Wandjina : aboriginal cave paintings in Kimberley, Western Australia, Oxford (1968).
18. V. J. Blundell, *Arctic Anthropol.* **11**, 213 (1974).
19. J. Huntleyet al., *Aust. Archaeol.* **78**, 33 (2014).
20. D. Paterson et al., *AIP Conf. Proc.* **1365**, 219 (2010).
21. C. G. Ryan et al., *J. Phys. Conf. Ser.* **499**, 12002 (2014).
22. D. L. Howard et al., *Anal. Chem.* **84**, 3278 (2012).
23. P. Dredge et al., *Appl. Phys. A Mater. Sci. Process.* **121**, 789 (2015).
24. L. Monico et al., *J. Anal. At. Spectrom.* **30**, 613 (2015).
25. M. Aubert et al., *Nature* **564**, 254 (2018).
26. R. S. Popelka-Filcoff et al., *Analyst* **141**, 3657 (2016).
27. P. Dredge et al., *Aust. New Zeal. J. Art* **17**, 147 (2018).
28. Frederick McCubbin, The North Wind at <https://www.ngv.vic.gov.au/ebooks/northwind/#/>
29. D. Thurrowgood et al., *Sci. Rep.* **6**, 29594 (2016). doi: 10.1038/srep29594
30. J. Divitcos et al., Proceedings: Mechanical Engineering Design of Synchrotron Radiation Equipment and Instrumentation Conf. (JACoW, Barcelona) **9,** 93–95 (2017). doi:10.18429/JACoW-MEDSI2016-MOPE38
31. G. Osmond et al., *Appl. Spectrosc.* **66**, 1136 (2012).
32. M. Donaldson and K. F. Kenneally, *Rock Art of the Kimberley: Proceedings of the Kimberley Society Rock Art Seminar Held at the University of Western Australia, Perth 10 September, 2005*, Kimberley Society (2007).